Tropical Animal Health and Production (2024) 56:223
https://doi.org/10.1007/s11250-024-04078-9

REGULAR ARTICLES

Surra-affected dromedary camels show reduced numbers of blood B-cells and in vitro evidence of *Trypanosoma*-induced B cell death

Jamal Hussen[1] · Hind Althagafi[2] · Mohammed Ameer Alalai[1] · Noof Abdulrahman Alrabiah[3] · Najla K. Al Abdulsalam[3] · Baraa Falemban[1] · Abdulaziz Alouffi[4] · Waleed S. Al-Salem[5] · Marc Desquesnes[6,7] · Laurent Hébert[8]

Received: 22 March 2024 / Accepted: 18 July 2024

Abstract

Trypanosomosis due to *Trypanosoma evansi* (surra) is one of the most important diseases with a significant impact on camel health and production. *Trypanosoma*-induced immunosuppression mechanisms, which are key factors of disease pathogenesis, have been characterized in several animal species. The present study investigated, therefore, the impact of trypanosomosis on the immunophenotype of blood leukocytes in camels. For this, the relative and absolute values of blood leukocyte populations, their expression pattern of cell surface molecules, and the numbers of the main lymphocyte subsets were compared between healthy camels and camels with clinical symptoms of chronic surra and serological evidence of exposure to *Trypanosoma* infection. Leukocytes were separated from the blood of healthy and diseased camels, labeled with fluorochrome-conjugated antibodies, and analyzed by flow cytometry. Compared to healthy camels, the leukogram of diseased camels was characterized by a slightly increased leukocyte count with moderate neutrophilia and monocytosis indicating a chronic inflammatory pattern that may reflect tissue injury due to the long-lasting inflammation. In addition, the analysis of lymphocyte subsets revealed a lower number and percentage of B cells in diseased than healthy camels. In vitro incubation of camel mononuclear cells with fluorochrome-labeled *T. evansi* revealed a higher capacity of camel B cells than T cells to bind the parasite in vitro. Furthermore, cell viability analysis of camel PBMC incubated in vitro with *T. evansi* whole parasites but not the purified antigens resulted in *Trypanosoma*-induced apoptosis and necrosis of camel B cells. Here we demonstrate an association between trypanosomosis in camels and reduced numbers of blood B cells. In vitro analysis supports a high potential of *T. evansi* to bind to camel B cells and induce their elimination by apoptosis and necrosis.

Keywords Trypanosomosis · Camel · Surra · B cells · Flow cytometry · Apoptosis

✉ Jamal Hussen
jhussen@kfu.edu.sa

[1] Department of Microbiology, College of Veterinary Medicine, King Faisal University, Al-Ahsa 31982, Al Hofuf, Saudi Arabia

[2] Biology Department, College of Science, Princess Nourah Bint Abdulrahman University, 11671 Riyadh, Saudi Arabia

[3] Department of Biological Sciences, College of Science, King Faisal University, Al-Ahsa 31982, Al Hofuf, Saudi Arabia

[4] King Abdulaziz City for Science and Technology, 12354 Riyadh, Saudi Arabia

[5] Ministry of Environment, Water and Agriculture, 11195 Riyadh, Saudi Arabia

[6] CIRAD, UMR INTERTRYP, 31076, Ecole Nationale Vétérinaire de Toulouse (ENVT), 23 Chemin Des Capelles, 31300 Toulouse, France

[7] INTERTRYP, Univ Montpellier, CIRAD, Montpellier, IRD, France

[8] ANSES, Laboratory for Animal Health, Normandy site, Physiopathology and Epidemiology of Equine Diseases (PhEED) Unit, ANSES, 1080 L'Église, 14430 Goustranville, France

Published online: 26 July 2024

Introduction

Camels are important livestock species with an estimated world population of more than 35 million head (Faye 2020). Camels have high economic value, especially in arid and semi-arid regions, due to their high thermotolerance being able to survive, reproduce, and produce milk and meat under harsh environmental conditions with limited food and water resources (Faye 2020).

Trypanosomosis represents one of the most important diseases of camels with significant impact on animal health and production due to reduced fertility, high losses in milk and meat production, and high mortality rates (Birhanu, et al. 2016). *Trypanosoma evansi (T. evansi)*, a member of the subgenus Trypanozoon (Oldrieve et al. 2021) is the most common cause of trypanosomosis in camels (Gerem et al. 2020; Tran et al. 2009). The parasite, which causes a disease known as surra, is the most widely distributed animal trypanosome (Birhanu, et al. 2016; Magez et al. 2021) affecting a wide range of species including camels, equines, dogs, and to a lesser extent cattle, sheep, goats, buffalo, elephants, deer, gazelles, and pigs (Desquesnes et al. 2013; Golombieski et al. 2023; Holland et al. 2003; Jawalagatti et al. 2023). In addition, recent studies that reported occasional *T. evansi* infections in humans, shed light on the zoonotic potential of the pathogen (Joshi et al. 2005; Powar et al. 2006; Shegokar et al. 2006; Van Vinh Chau et al. 2016, World Health Organization 2005). In camels, the disease course takes most commonly a chronic form that can last several years leading to reduced fertility and generalized loss of body condition. The clinical symptoms typically include appetite and weight loss, muscular atrophy and drooped hump, general weakness with slow and short distance walking, lacrimation, anemia with pale mucous membranes, petechial haemorrhages, oedema in different body areas, and neurological symptoms (Desquesnes, et al. 2013)(Wilson and Dioli 2021).

Direct diagnosis of surra is based on the detection of the parasite by microscopic analysis of Giemsa-stained blood smears or the demonstration of actively moving parasites in concentrated hematocrit tubes preparations; infection can also be objected by the detection of parasite genetic material in buffy coat samples by PCR (Kim et al. 2023). Besides these agent detection methods, serological evidence of exposure to *T. evansi* can be brought by the detection of anti-*Trypanosoma* antibodies in camel serum. For this, the card agglutination test for *T. evansi* (CATT/*T. evansi*) and the enzyme-linked immunosorbent assay (ELISA) for *T. evansi* can be used (Tran, et al. 2009).

Innate immune response against trypanosomes is mediated by activation of the complement system and early induction of the inflammatory cytokine interferon (IFN) gamma by innate lymphocytes leading to activation of macrophages and enhancement of their killing potential (Baral et al. 2007; Engstler et al. 2007; Harris et al. 2007). The adaptive immune response to the parasite is characterized by an early production of IgM antibodies that target the mannose-rich residues of the VSG coat followed by IgG production; the IgGs are directed against the N-terminal epitopes of VSG with IgM having the superior role over IgG in parasitemia control (Nguyen et al. 2021). In their mammalian host, trypanosomes are known for their strategies to escape the host's innate and adaptive immune responses (Magez, et al. 2021). In addition to evading the antibody-mediated destruction through the continuous switch of their surface antigenic coat, trypanosomes induce loss in distinct immune cell populations from their host. Studies in a mouse model for *T. brucei*, another Trypanozoon member, revealed that especially the infection-induced depletion of several B cell subsets renders the host unable to mount a protective humoral immune response (Radwanska et al. 2008).

In the dromedary camel, although several studies evaluated the serologic response to *T. evansi* (Al-Harrasi et al. 2023; Habeeba et al. 2022), the impact of infection on the cellular immune system has not been investigated so far. The present study compared the immunophenotype of blood leukocytes in *T. evansi* serologically positive and negative camels. In addition, in vitro stimulation studies were performed to explore the mechanisms behind the observed changes in leukocyte composition. Given the lack of effective vaccines against the disease, such studies will support a better understanding of host-pathogen interaction mechanisms in camel trypanosomosis, paving the way for the development of effective control strategies.

Materials and methods

Animals

Fifty-five animals, including thirty diseased and twenty-five healthy dromedary camels (*Camelus dromedarius*), were involved in the present study. The study was conducted between January 1, 2022 and June 30, 2023. The diseased camels originated from 5 different camel herds in the eastern province of Saudi Arabia. The diseased animals were brought to the KFU Veterinary Teaching Hospital (King Faisal University in Al-Ahsa, Saudi Arabia) with symptoms compatible with the chronic form of camel trypanosomosis (Surra). The healthy camels were selected from the animals reared on the camel farm of the Camel Research Center at King Faisal University. All camels in the healthy and diseased group were from the black Almajaheem camel breed. For all camels, clinical examination was performed

by a trained veterinarian. The majority of diseased camels showed signs of weakness, inappetence, emaciation, muscle atrophy, hollow left flank, and retracted abdomen due to anorexia, pale mucous membrane of the conjunctiva, and lacrimation. In addition, some camels showed edema, urticaria plaques, and thinning of the hump and dropping it to one side. Abortion with elevation of body temperature was observed only in one camel (Supplementary Table 1). The control animals were clinically healthy with no signs of injury or disease (respiratory or gastrointestinal disease, mastitis, or metritis) and had no history of any *T. evansi* infection.

Collection of serum and whole blood samples

Blood samples were collected by venipuncture of the jugular vein (vena jugularis externa) into clot activator vacutainer tubes for serum collection and into BD Vacutainer™ K3EDTA Tubes for collection of whole blood samples. Serum samples were collected after centrifugation of the tubes for 15 min at × 1000 g and stored at -20°C for further analysis.

Parasitological examination

Thin blood smears were prepared from fresh whole blood followed by air-drying, fixation in absolute methanol, and staining with Giemsa's stain. Stained smears were examined for trypanosomes with a light microscope using × 40 magnification and oil immersion objective (Gerem, et al. 2020).

Whole-cell lysate antigen ELISA

The detection of antibodies to pan-trypanosome antigens was performed by ELISA-PanTryp, using *T. evansi* WCLAs in a protocol derived from Bossard & Desquesnes (Bossard and Desquesnes 2023). Briefly, 96 well NUNC Maxisorp plates were coated with 100 µL of the whole cell lysate antigen (WCLA) at a concentration of 5 µg/mL in 0.05 M carbonate-bicarbonate buffer, pH 9.6. After incubation overnight at 4 °C, the plate was emptied by reversion, and 150 µL blocking buffer (PBS containing 1% bovine serum albumin and 0.008% tween 20) was added to the plate followed by incubation for 30 min at 37 °C with shaking at 300 rpm. After blocking, the plate was washed three times with washing buffer (PBS containing 0.1% Tween 20). Positive and negative camel control sera and test serum samples were diluted 1:100 in blocking buffer and 100 µL of diluted serum were added to the plate in duplicates. After incubation for 30 min at 37 °C with shaking at 300 rpm, the plate was washed three times with washing buffer. After that 100 µL of Protein A conjugated with horseradish peroxidase diluted 1:10,000 in blocking buffer were added to each well. After incubation for 30 min at 37 °C with shaking at 300 rpm, the plate was washed three times before adding 100 µL per well of the 3, 3′,5,5′-Tetramethylbenzidine (TMB) substrate solution followed by incubation for 30 min at RT in the dark. Finally, the reaction was stopped by the addition of 0.2 M sulfuric acid followed by reading at 450 nm using the IMARK ELISA reader (Bio-Rad Laboratories GmbH, Munich, Germany). The results were expressed as the percentage ratio of the positive control serum (Relative percentage of positivity; RPP) by dividing the corrected mean OD value of test serum (after subtracting the mean OD value of negative control serum) by the corrected OD value of the positive control serum (after subtracting the OD value of the negative control serum). Samples with an RPP ≥ 20% were considered positive (Bossard and Desquesnes 2023). The WCLA and the positive and negative camel sera were purchased from CIRAD, IRD, Montpellier, France. The ELISA plates, coating buffer, BSA, Protein A conjugate, and the substrate and stop solutions were from Sigma-Aldrich.

Cell separation from camel blood

For all healthy and diseased camels, leukocytes were isolated from EDTA blood by centrifugation after hypotonic lysis of red blood cells (RBC). For this, 5 mL *aqua dest* was added to 2 mL blood for 20 s followed by the addition of 5 mL of 2 × phosphate buffered saline (PBS). After centrifugation for 15 min at 1000 × g in a cooled centrifuge (4 °C), the supernatant containing the lysed RBC was removed and the pellet was gently resuspended. This step was repeated three times with centrifugation at 500 × g and 250 × g. Finally, the WBC pellet was suspended in PBS containing 1% BSA and sodium azide (MIF buffer) and adjusted to 5×10^6 cells/mL. The propidium iodide (PI) exclusion assay was used to check the viability of separated cells. For all experiments involving cell staining and flow cytometry, cell viability was higher than 96% (Supplementary Fig. 1).

Peripheral blood mononuclear cells (PBMCs) were separated from buffy-coat blood by density gradient centrifugation over *Lymphoprep*™ (STEMCELL Technologies, Vancouver, Canada). For this, 5 mL blood was diluted 1:2 with phosphate buffered saline (PBS) and the mixture was layered on 5 mL of *Lymphoprep*™ in a 15 mL sterile falcon tube. After centrifugation at 4℃ for 30 min at 800 × g without break, the PBMC-containing interphase was collected carefully using a 10 mL pipette. After three washes in cold PBS (400 × g, 200 × g, 100 × g for 10 min at 4℃), the cells were counted, and suspended in RPMI culture medium at 2×10^6 cells / mL.

Labeling of cells with monoclonal antibodies

For the immunophenotyping of blood leukocytes, separated cells were incubated in a round-bottomed 96-well plate for 15 min at 4℃ with a combination of unlabeled monoclonal antibodies (mAbs) to cell surface molecules (Table 1 and Table 2). In the second step and after washing (two times) with cold MIF buffer for 3 min at 300 × g and 4℃, the cell pellet was resuspended and incubated for 15 min at 4℃ with a combination of secondary antibodies against mouse IgM, IgG1, and IgG2a (Life Technologies, California, USA). Finally, the cells were washed two times with cold MIF buffer for 3 min at 300 × g and 4℃ and the cell pellet was resuspended in MIF buffer for flow cytometry.

For the experiments with separated camel PBMCs, cells were incubated in a round-bottomed 96-well plate for 15 min at 4℃ with a combination of the following monoclonal antibodies (mAbs) in a two-step staining procedure: mouse IgM against the cluster of differentiation (CD)4, mouse IgG1 against the workshop cluster (WC)1, and mouse IgG2a against the major histocompatibility complex (MHC) class II molecules (all from Kingfisher Biotech, Minnesota, USA). In the second step and after washing (two times) with cold MIF buffer for 3 min at 300 × g and 4℃, the cell pellet was resuspended and incubated for 15 min at 4℃ with a combination of an APC-conjugated goat IgG antibody against mouse IgM, PE-conjugated goat IgG antibody against mouse IgG2a, and FITC-conjugated goat IgG antibody against mouse IgG1 (Life Technologies, California, USA). Finally, the cells were washed two times with cold MIF buffer for 3 min at 300 × g and 4℃ and the cell pellet was resuspended in RPMI medium for further analysis.

In vitro incubation of camel PBMCs with *T. evansi*

A freeze-dried suspension of inactivated, purified, and fixed trypanosomes of the Variable Antigen Type (VAT) Rode Trypanozoon antigen type (RoTat) 1.2 (WOAH (formerly OIE)-Reference Laboratory for surra, Institute of Tropical Medicine, Antwerp, Belgium) was reconstituted with 1 mL PBS and the suspension was labeled (incubation for 5 min at RT) with 7-Aminoactinomycin D

Table 1 List of antibodies

Antigen	Antibody clone	Target species	Labeling	Source	Isotype
CD45	LT12A	Llama	-	Kingfisher	Mouse IgG2a
CD44	LT41A	Llama	-	Kingfisher	Mouse IgG2a
CD14	CAM36A	Camel	-	Kingfisher	Mouse IgG1
MHCII	TH81A5	Swine	-	Kingfisher	Mouse IgG2a
CD172a	DH59b	Bovine		Kingfisher	Mouse IgG1
CD163	LND68A	Bovine	-	Kingfisher	Mouse IgG1
CD4	GC50A1	Bovine	-	VMRD,	Mouse IgM
WC1	BAQ128A	Bovine	-	VMRD,	Mouse IgG1
CD18	6.7	Human	FITC	BD	Mouse IgG2a
Mouse IgM	poly	Mouse	APC	Thermofisher	Goat IgG
Mouse IgG1	poly	Mouse	FITC	Thermofisher	Goat IgG
Mouse IgG2a	poly	Mouse	PE	Thermofisher	Goat IgG

MHC Major Histocompatibility Complex, *WC1* workshop cluster 1, *APC* Allophycocyanin, *FITC* Fluorescein isothiocyanate, *PE* Phycoerythrin, *poly* polyclonal. Reactivity with camel leukocyte antigens was reported in previous studies (Hussen and Schuberth 2020)

Table 2 Staining combinations

Combination	Primary antibody cocktail	Secondary antibody cocktail
1	CD45 / CD172a	Mouse IgG1-FITC / Mouse IgG2a-PE
2	CD4 / WC1	Mouse IgG1-FITC / Mouse IgM-APC
3	CD14 / MHCII	Mouse IgG1-FITC / Mouse IgG2a-PE
4	CD163 / CD44	Mouse IgG1-FITC/ Mouse IgG2a-PE
5	CD18-FITC	
6	-	Mouse IgG1-FITC / Mouse IgG2a-PE / Mouse IgM-APC

MHC Major Histocompatibility Complex, *WC1* workshop cluster 1, *APC* Allophycocyanin, *FITC* Fluorescein isothiocyanate, *PE* Phycoerythrin

(7-AAD), a fluorescent dye with strong affinity for DNA which only penetrates the membrane of dead cells (in this case the fixed *T. evansi* parasites) and undergoes a spectral shift upon association with DNA. It is used as a fluorescent marker for DNA in place of propidium iodide (PI) with the advantage of its ability to be used with phycoerythrin (PE)- and fluorescein isothiocyanate (FITC)-labeled monoclonal antibodies in 2-color analysis, with minimal spectral overlap. After washing with cold PBS for 10 min, the labeled parasites were suspended in RPMI medium, counted on the flow cytometer (Accuri C6; BD), and adjusted to 4×10^6 parasites / mL (Barr et al. 2021; McGrath et al. 2017). Purified and antibody-labeled camel PBMCs were incubated in vitro with 7-AAD-labeled *T. evansi* for 30 min at 37 °C and 5% CO_2. For this, 1×10^5 cells (in 50 µL RPMI medium) were added to 50 µL RPMI medium containing 1×10^5 trypanosomes in the wells of a 96-well sterile cell culture plate. Control cells were incubated in medium alone.

Cell vitality assay

Cell vitality was measured by flow cytometry using the Annexin V-FITC Apoptosis Kit according to the kit protocol (Abcam; ab14085). The washed cell pellet of stimulated and non-stimulated cells was stained in cell culture plates (96-wells) with Annexin V-FITC and propidium iodide (PI) diluted 1:100 in KIT buffer (100 µL /well) for 5 min at RT in the dark. Cells were classified upon excitation at 488 nm into Annexin V + /PI- apoptotic cells, Annexin V + / positive/PI + necrotic cells, and Annexin V-/PI- (Hussen et al. 2023a).

Statistical analyses

Data normality, mean, and standard error of the mean (SEM) were measured using the column statistics function in combination with the Shapiro–Wilk normality test of the statistical program Prism (GraphPad Software V5, California, USA). For the comparison between two groups, the unpaired two-tailed T-test was used for normally distributed data, and the Mann–Whitney test was used if either one or both group's data was not normally distributed. For the comparison between data from more than two groups, the one-factorial analysis of variance (ANOVA) with *Bonferroni's* correction was used for normally distributed data, while the *Kruskal–Wallis test* was used with the *Dunn's Multiple Comparison test* for comparison between not normally distributed data. Differences were considered significant if the P value was less than 0.05.

Results

Clinical disease and serological findings

All camels with clinical symptoms of surra were found sero-positive for *T. evansi* using the WCLA-based indirect ELISA, while anti-*Trypanosoma* antibodies were only detected in one out of the 25 clinically healthy camels (Fig. 1A, Table 3). The parasite could be detected in only one animal by microscopic analysis of Giemsa-stained blood smear. Only one animal from the healthy group tested positive using the WCLA ELISA. In the WCLA ELISA, the healthy camel group showed a mean RPP of 9.3% ± 1.4 compared to 37.7% ± 3.3 in the diseased group ($P < 0.01$). The antibody level (RPP) of individual camels within the seropositive group ranged between 22

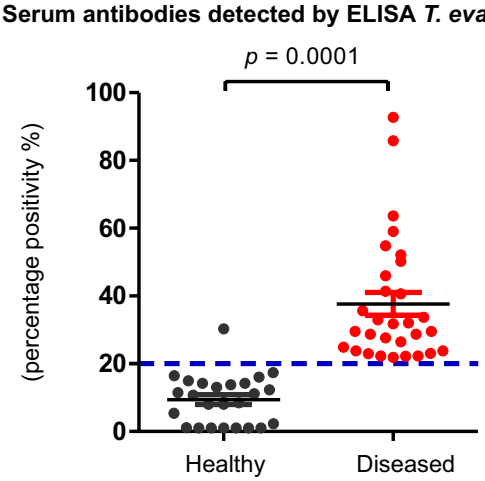

Fig. 1 Serum level of antibodies to the whole cell lysate antigen (WCLA) of *T. evansi*. Serum samples collected from clinically healthy (n = 25) dromedary camels and camels with clinical symptoms of surra (n = 30 animals) were tested for antibodies to the WCLA using ELISA. For each serum, the antibody level was expressed as the relative positivity percentage (RPP) of the positive control serum. A blue dotted line was drawn to indicate the cut-off value. Healthy camel sera were presented in black, while those of diseased camels were presented in red. *P* values were calculated using the student's *T*-test

Table 3 Serological results

Animal group	Gender		Age	WCLA ELISA	
	Male	Female	Mean ± SEM	+	-
Healthy (25)	2	23	8.7 ± 0.8	1	24
Diseased (30)	3	27	7.9 ± 0.8	30	0

WCLA Whole cell lysate antigen

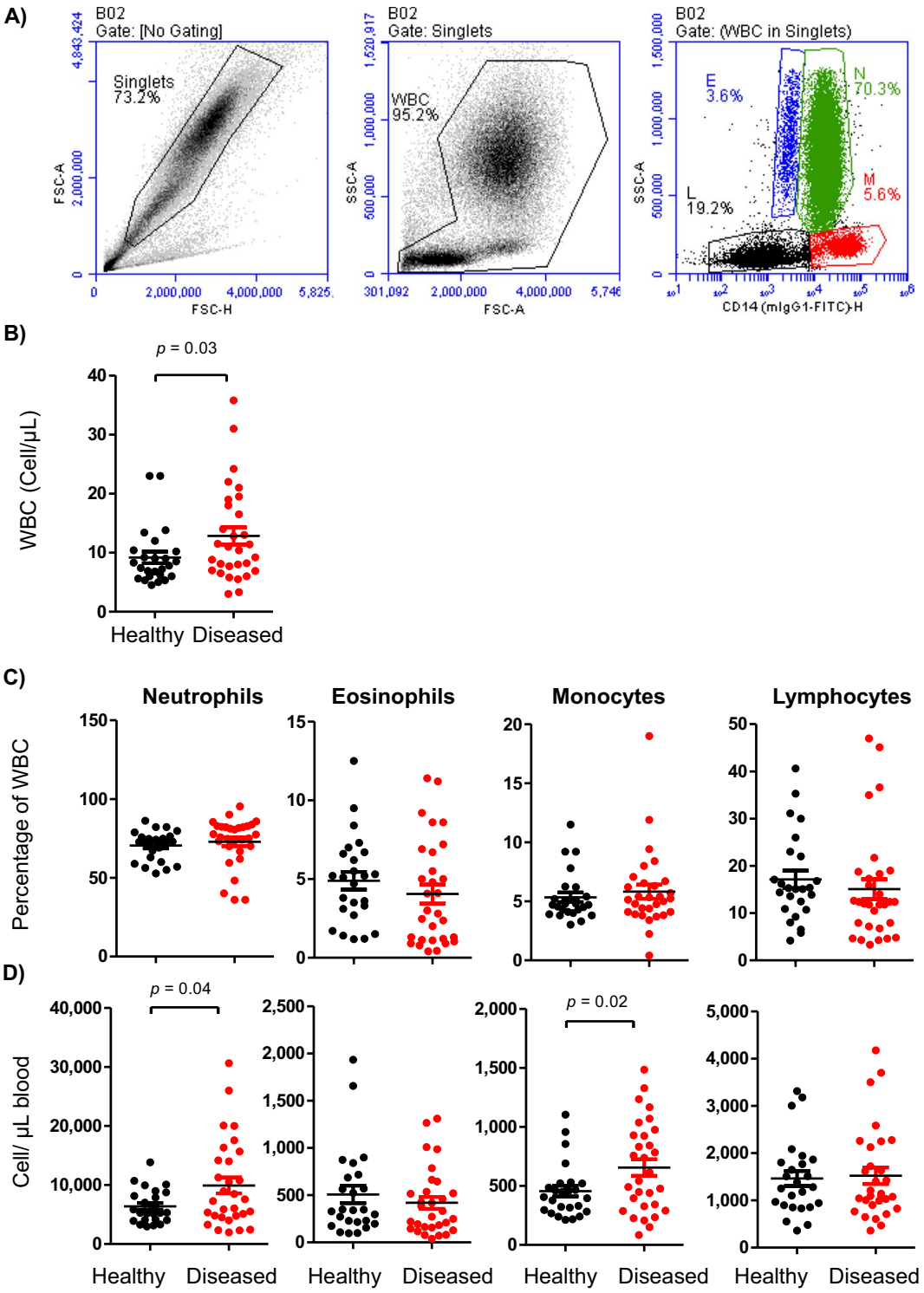

Fig. 2 Identification and enumeration of total leukocytes and their subpopulations in blood from healthy and diseased camels. Leukocytes were separated from blood and labeled with antibodies to CD14. (**A**) After gating on singlets (using FSC height (FSC-H) against FSC area (FSC-A) dot plot) and defining the leukocyte population (based on FSC and SSC signals), eosinophils (E), granulocytes (G), monocytes (M), and lymphocytes (L) were gated based on their staining with CD14 antibodies and SSC characteristic. Total cell count of leukocytes (**B**), the percentages (**C**)**,** and the absolute numbers (**D**) of eosinophils, granulocytes, monocytes, and lymphocytes were calculated for healthy and diseased camels and presented as scattered plot graphs and *p* values less than 0.05 according to the student's *T*-test were indicated

and 93 (Supplementary Table 1). The positive animals were classified into a low (RPP ≥ 20 and < 30) and a high (RPP ≥ 30) seropositive group with a mean antibody level of 24.7 ± 0.9 and 48.8 ± 4.8, respectively. No differences in the severity grade of the clinical symptoms could be identified between the low and the high seropositive camels. As no molecular test was used for the identification of the agent, the classification of animals as healthy and diseased is based on the clinical symptoms and supported by the serology.

Leukocyte composition in healthy and diseased camels

Flow cytometric analysis (Fig. 2A) was used in combination with absolute counting to calculate the relative and absolute numbers of leukocyte populations (Table 4). The diseased animal group (12.8 ± 1.4) showed a significantly (P = 0.03) higher total leukocyte count (Fig. 2B) in their blood compared to the healthy group (9.4 ± 1.0). Differential leukocyte count revealed no significant differences (p > 0.05) in the relative leukocyte composition with comparable percentages of neutrophils, eosinophils, monocytes, and lymphocytes between the two groups (Fig. 2C). The diseased group, however, showed significantly (p < 0.05) higher numbers of neutrophils (10.0 ± 1.3 × 10^3 cell/µL) and monocytes (0.65 ± 0.06 × 10^3 cell/µL) in their blood than the neutrophils (6.8 ± 0.8 × 10^3 cell/µL) and monocyte (0.45 ± 0.04 × 10^3 cell/µL) count in blood of the healthy group (Fig. 2D).

Lymphocyte composition in healthy and diseased camels

Flow cytometric analysis of lymphocyte composition (Fig. 3A) revealed a significantly lower ($P = 0.02$) fraction of B lymphocytes in the blood of the diseased animals (14.1 ± 0.9% of lymphocytes) compared to the healthy animals (17.8 ± 1.5% of lymphocytes), while no significant differences in the percentages of helper and γδ T cells were observed between the two groups (Fig. 3B). Similarly, the absolute count of B lymphocytes was significantly ($P = 0.02$) lower in the blood of the diseased animals (183.4 ± 22.0 cell/µL) compared to the healthy (277.9 ± 41.1 cell/µL) animals (Fig. 3B). Neither the percentages nor absolute counts of helper T cells or γδ T cells showed significant differences between the two groups (Fig. 3B-C and Table 4).

Immunophenotype of leukocyte subsets

Immunophenotyping of monocytes revealed significantly ($P = 0.04$) higher abundance of the major histocompatibility complex (MHC) molecule class II on the surface of

Table 4 WCLA antibody level and leukocyte immunophenotype in healthy and diseased camels

		Healthy N = 25	**Diseased** N = 30	**WCLA-Ab titer in diseased camels**			
					Low (n = 15) (20 < PP < 30)	*High (n = 15) (RPP ≥ 30)*	***P value***
WCLSA antibody level		9.3 ± 1.4	37.7 ± 3.3	***P < 0.01***	*24.7 ± 0.9*	*48.8 ± 4.8*	***P < 0.01***
Leukocyte populations (× 10^3/µL)	WBC	9.4 ± 1.0	12.8 ± 1.4	***P = 0.03***	11.9 ± 2.0	13.8 ± 1.5	*P = 0.25*
	PMN	6.8 ± 0.8	10.0 ± 1.3	***P = 0.03***	8.7 ± 1.6	11.1 ± 2.0	*P = 0.36*
	Eos	0.51 ± 0.10	0.42 ± 0.06	*P = 0.22*	0.33 ± 0.08	0.51 ± 0.09	*P = 0.14*
	Mon	0.45 ± 0.04	0.65 ± 0.06	***P = 0.01***	0.67 ± 0.09	0.61 ± 0.10	*P = 0.52*
	Ly	1.46 ± 0.17	1.52 ± 0.17	*P = 0.39*	1.71 ± 0.29	1.31 ± 0.15	*P = 0.23*
Leukocyte populations (% of WBC)	PMN	70.6 ± 1.9	72.8 ± 2.7	*P = 0.49*	68.6 ± 4.7	77.2 ± 2.0	***P = 0.04***
	Eos	4.9 ± 0.6	4.0 ± 0.6	*P = 0.17*	2.9 ± 0.6	5.3 ± 1.0	***P = 0.04***
	Mon	5.4 ± 0.4	5.8 ± 0.6	*P = 0.28*	6.7 ± 1.0	4.8 ± 0.5	*P = 0.11*
	Ly	17.2 ± 1.9	15.1 ± 1.9	*P = 0.22*	18.1 ± 3.6	11.8 ± 1.4	***P = 0.04***
	NLR	5.3 ± 0.7	9.1.2 ± 1.9	***P = 0.01***	9.0 ± 1.9	8.9 ± 1.6	*P = 0.43*
Ly. sub (cell/ µL)	CD4	272.7 ± 28.7	275.0 ± 25.1	P = 0.93	324.3 ± 41.4	222.5 ± 21.4	***P = 0.04***
	WC1	94.8 ± 16.3	137.0 ± 29.6	*P = 0.10*	120.9 ± 35.0	154.2 ± 49.5	P = 0.58
	B cell	277.9 ± 41.1	183.4 ± 22.0	***P = 0.02***	180.2 ± 39.1	186.2 ± 22.3	*P = 0.90*
Ly. sub. %	CD4	19.3 ± 1.6	19.8 ± 1.2	*P = 0.38*	21.6 ± 1.9	17.9 ± 1.3	*P = 0.12*
	WC1	6.3 ± 0.7	8.4 ± 1.3	*P = 0.07*	6.3 ± 1.9	10.6 ± 2.4	*P = 0.11*
	B cell	17.8 ± 1.5	14.1 ± 0.9	***P = 0.02***	13.8 ± 1.4	14.4 ± 1.2	*P = 0.75*

RPP Relative percent positivity indicates the anti-*trypanosoma* antibody level as measured by ELISA, *WBC* white blood cells, *PMN* neutrophils, *Eos* eosinophils, *Mon* monocytes, *Ly* lymphocytes, *Sub* subsets,values presented as Mean ± SEM; *p* values in bold indicates significant differences between the groups (*t*-test)

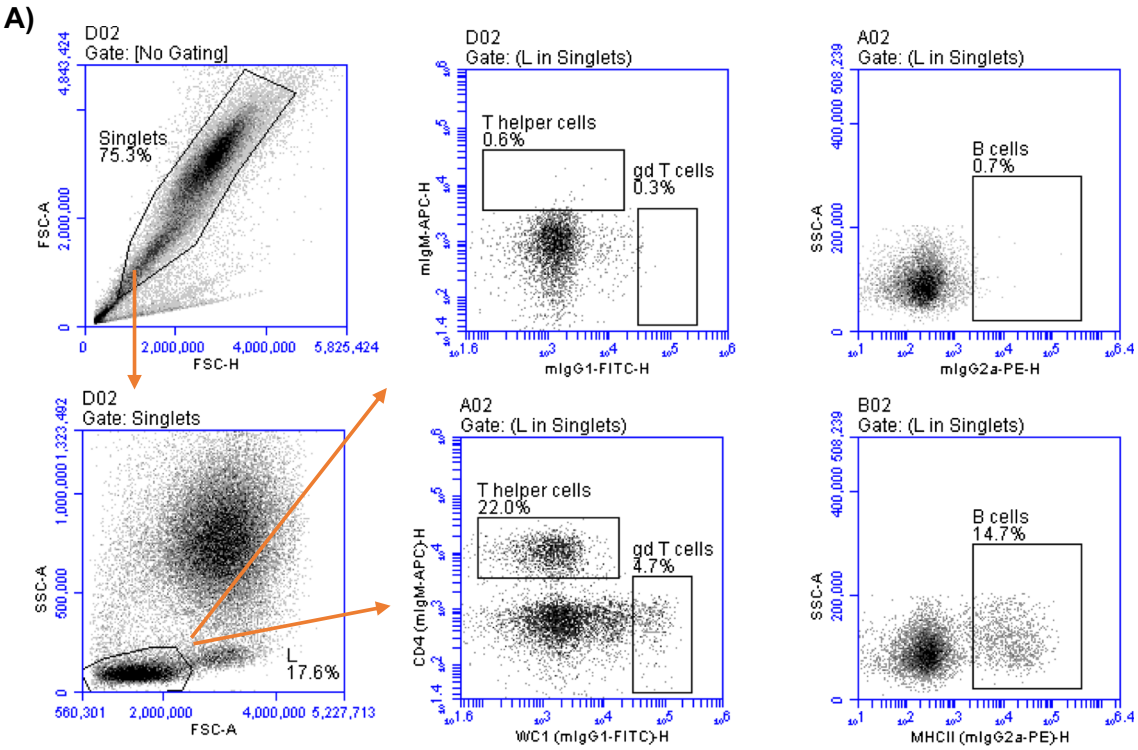
A)
D02
Gate: [No Gating]
Singlets
75.3%
FSC-A
FSC-H
D02
Gate: (L in Singlets)
T helper cells
0.6%
gd T cells
0.3%
mIgM-APC-H
mIgG1-FITC-H
A02
Gate: (L in Singlets)
B cells
0.7%
SSC-A
mIgG2a-PE-H
D02
Gate: Singlets
L
17.6%
SSC-A
FSC-A
A02
Gate: (L in Singlets)
T helper cells
22.0%
gd T cells
4.7%
CD4 (mIgM-APC)-H
WC1 (mIgG1-FITC)-H
B02
Gate: (L in Singlets)
B cells
14.7%
SSC-A
MHCII (mIgG2a-PE)-H

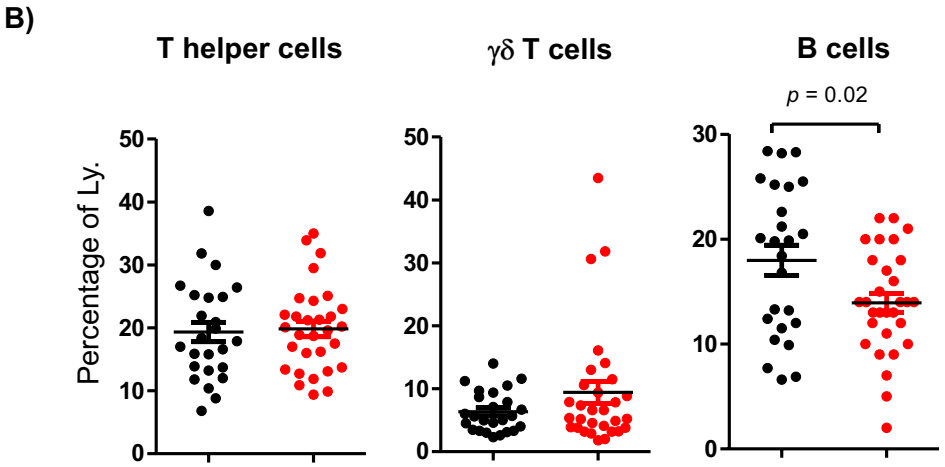
B)
T helper cells
γδ T cells
B cells
p = 0.02
Percentage of Ly.

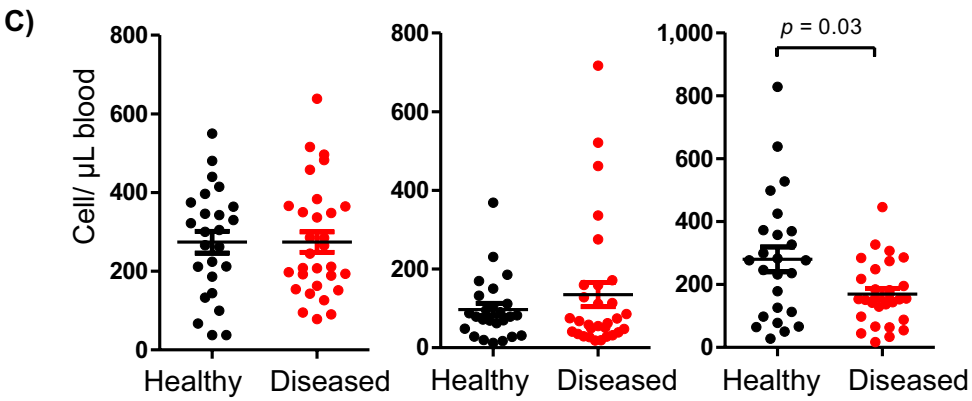
C)
p = 0.03
Cell/ µL blood
Healthy
Diseased
Healthy
Diseased
Healthy
Diseased

◂**Fig. 3** Identification and enumeration of lymphocyte subsets in blood from healthy and diseased camels. Leukocytes were separated from blood and labeled with antibodies to CD4, WC1, and MHCII or with corresponding isotype controls and analyzed by flow cytometry. (**A**) After gating on singlets and defining the lymphocyte (L) population (based on FSC and SSC signals), T helper cells, γδ T cells, and B cells were identified based on their staining with CD4, WC1, and MHCII, respectively (representative dot plots showing positive staining and isotype control staining). The percentages (**B**) and the absolute numbers (**C**) of lymphocyte subsets were calculated for healthy (black dots) and diseased (red dots) camels and presented as scattered plot graphs and p values less than 0.05 according to the student's *T*-test were indicated

monocytes from the diseased animal group (14,654 ± 1427 MFI) compared to the healthy (10,729 ± 1150 MFI) animal group (Fig. 4A). The expression densities of the monocyte markers CD14 and CD163, the myeloid marker CD172a, or the cell adhesion molecules CD45, CD44, and CD18 did not differ significantly ($p > 0.05$) between the two groups (Fig. 4A).

The phenotype of blood neutrophils from the diseased group was characterized by lower expression density of the cell adhesion molecule CD18 when compared to the healthy group (21,238 ± 885 MFI versus 23,464 ± 549 MFI in the healthy group), while the expression of CD14, MHCII, CD45, or CD44 did not differ significantly between the two groups (Fig. 4B).

For blood lymphocytes, the cell adhesion molecules CD44 and CD45 were significantly ($P = 0.04$ and $p = 0.04$ for CD45) higher expressed on lymphocytes from the diseased (33,065 ± 1291 MFI for CD44 and 53,487 ± 2500 for CD45) compared to the healthy group (29,210 ± 1395 MFI and 45,180 ± 3026 for CD45), while no significant differences in the expression of CD18 were observed between the two groups (Fig. 4C).

Impact of anti-*trypanosoma* antibody level on the immunophenotype of leukocytes

The comparison between the animals with low and high antibody levels revealed higher percentages of neutrophils and eosinophils but a lower percentage of lymphocytes compared to the low antibody level group. The absolute counting, however, did not show significant differences between the two groups (Table 4). In addition, with the exception of lower number of helper T cells in the high group, the low and high antibody level groups did not show significant differences regarding their lymphocyte composition or the expression density of surface markers on their monocytes, neutrophils, or lymphocytes.

Binding of *T. evansi* to camel lymphocyte subpopulations

Incubation of mononuclear cells (PBMCs) separated from healthy camels with inactivated (formalin-fixed) and 7-AAD-labeled *T. evansi* revealed different capacities of lymphocyte subpopulations to bind to *T. evansi*. Camel B cells and T cells were identified as small SSC^{low}/FSC^{low} lymphocytes based on the differential expression of MHCII. Camel helper T cells, γδ T cells were identified based on the expression of CD4 and WC1 surface antigens. T cell subsets other than helper T cells and γδ T cells were identified as $CD4^{-}MHCII^{-}WC1^{-}$ lymphocytes (Fig. 5A). Within lymphocytes, B cells showed the highest ($p < 0.05$) binding capacity (measured as the mean fluorescence intensity of cell staining with *T. evansi*-7-AAD) to *T. evansi* (Fig. 5B). The binding of *T. evansi* to camel monocytes was, however, higher ($p < 0.05$) than all lymphocyte subpopulations (Fig. 5C).

In vitro stimulation with *T. evansi* selectively induced cell death in camel B cells

The impact of *T. evansi* stimulation on cell vitality of camel lymphocyte subpopulations was evaluated by flow cytometric measurement of cell apoptosis and necrosis in camel B cells (Fig. 6 A) and T cells (Fig. 6 B). Spontaneous cell death (measured in cells incubated in medium) resulted in a percentage of 6.3 ± 0.2% and 4.5 ± 0.2% apoptotic cells within total B cells and T cells, respectively (Fig. 6C), while the percentage of necrotic cells was 3.7 ± 0.2% and 0.9 ± 0.1% of total B cells and T cells, respectively (Fig. 6D). Incubation with *T. evansi* significantly ($p < 0.05$) increased the percentage of apoptotic cells (13.5 ± 0.2%) and necrotic cells (4.9 ± 0.2%) within total B cells, while incubation with the purified *T. evansi* Ro Tat 1.2 antigen did not affect ($p > 0.05$) B cell apoptosis (5.9 ± 0.4%) or necrosis (3.8 ± 0.1%). Neither incubation with *T. evansi* nor with the purified RoTat 1.2 antigen affected cell apoptosis or necrosis of T cells ($p > 0.05$) when compared to incubation in medium control alone (Fig. 6C and 6D).

Discussion

African trypanosomes of the Trypanozoon sub-genus are extra-cellular parasites responsible for infections in several livestock species. In their host species, trypanosomes are

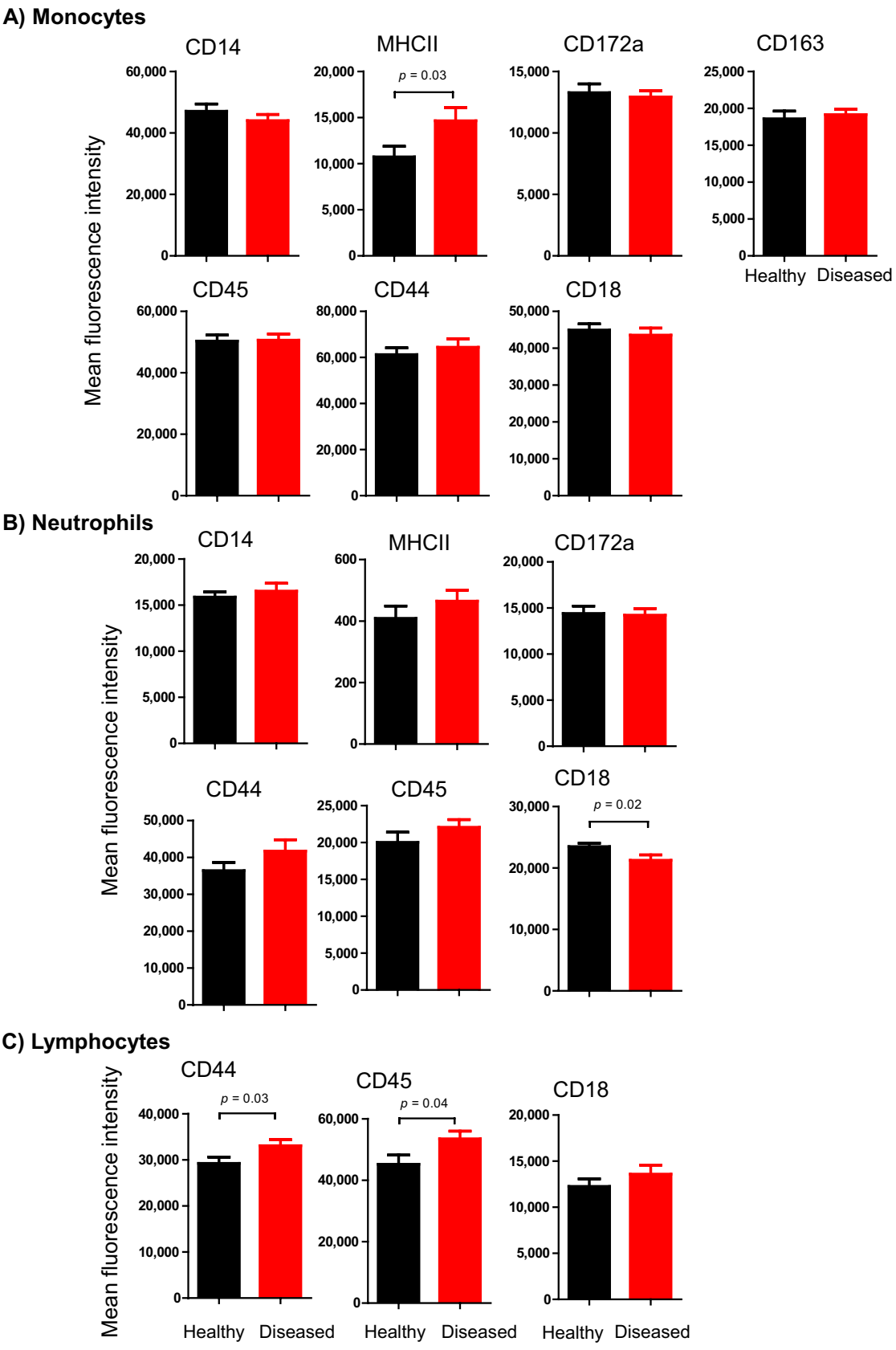
A) Monocytes
CD14
MHCII
CD172a
CD163
p = 0.03
Mean fluorescence intensity
Healthy
Diseased
CD45
CD44
CD18
B) Neutrophils
CD14
MHCII
CD172a
Mean fluorescence intensity
CD44
CD45
CD18
p = 0.02
C) Lymphocytes
CD44
CD45
CD18
p = 0.03
p = 0.04
Mean fluorescence intensity
Healthy
Diseased
Healthy
Diseased
Healthy
Diseased

◂**Fig. 4** Phenotype of leukocyte populations in healthy and diseased camels. Separated leukocytes were stained with monoclonal antibodies to some cell surface molecules and analyzed by flow cytometry. The abundance of myeloid markers and cell adhesion molecules was measured on monocytes (**A**) and neutrophils (**B**). For lymphocytes (**C**) only the abundance of the cell adhesion molecules was measured. For each molecule, the mean fluorescence intensity (MFI) was measured and presented graphically as Mean ± SEM for healthy and diseased camels. *P* values less than 0.05 according to the student's *T*-test were indicated

known for their immune evasion strategies (Dos Santos et al. 2020; Pays et al. 2023). In camels, although trypanosomosis is a serious disease challenging camel health and production due to the high impact on productivity and the disease-associated economic losses (Ogolla et al. 2023; Rottcher et al. 1987; Salim et al. 2011), studies on the impact of trypanosomosis on the camel immune system are rare. The present study investigated, therefore, the impact of camel trypanosomosis on the immunophenotype of blood leukocytes. For this, the relative and absolute values of blood leukocyte populations, their expression pattern of cell surface molecules, and the numbers of the main lymphocyte subsets were compared between healthy camels and camels with clinical symptoms for chronic surra and serological evidence of exposure to *Trypanosoma* infection.

In the present study, the high positivity of the ELISA test, which detects IgG antibody isotypes, together with the low parasitological detection within animals with clinical symptoms, indicate the chronic nature of infection with low parasitaemia levels in the diseased animals. In addition, the clinical signs of emaciation, anorexia, thinning of the hump, anemia, and abdominal oedema are consistent with chronic trypanosomosis (Wilson and Dioli 2021).

Although the whole cell lysate antigen ELISA was able to identify antibodies in all camels with clinical symptoms, the results of the present study is limited by the lack of differentiation between past and current infections which requires the employment of parasites molecular detection tests like the polymerase chain reaction (PCR) (Tran, et al. 2009).

In the present study, the observed leukocytosis with neutrophilia in the diseased animal group indicates an inflammatory leukogram pattern (Hussen and Schuberth 2020). In addition, the increased numbers of monocytes in the blood of the diseased animals, which may or may not be part of an inflammatory leukogram, is usually indicative for tissue injury due to long-lasting inflammation. It could be a result of increased production of monocytes in the bone marrow to replenish tissue macrophages for resolving the inflammation (Soehnlein and Lindbom 2010). Their enhanced expression of MHCII, a marker of inflammatory monocytes and macrophages, reflects an early polarization of these circulatory cells toward a classically activated M1 macrophage phenotype. This seems in agreement with the recently reported phenotype of monocyte-derived macrophages generated in vitro under the effect of *T. evansi* antigens (AL_Hilal et al. 2023).

As extracellular blood pathogens, the continued exposure of parasites from the trypanozoon sub-genus to antibody-mediated destruction demonstrates the protective role of B cell-mediated humoral immune response (Onyilagha and Uzonna 2019; Otesile and Tabel 1987). Using fluorochrome-labeled *T. evansi*, the present study confirmed the high binding potential between camel monocytes and *T. evansi* (Hussen et al. 2023b) and revealed a higher capacity of camel B cells than T cells to bind the parasite in vitro, indicating the key role of B cells in the early interaction with the pathogen. In support of this is the marked difference in the B cell count between healthy and diseased animals with a lower percentage and absolute count of B cells in the blood of diseased compared to healthy animals. This seems in agreement with the destructive effect of trypanosomes on B lymphocytes reported in other species (Bockstal et al. 2011; Dos Santos, et al. 2020; Obishakin et al. 2014; Onyilagha and Uzonna 2019; Radwanska, et al. 2008). In an experimental multi-wave chronic *T. brucei* infection in mice, a recent study focused on the analysis of the splenic marginal zone B cells, which are responsible for protective antibody response to the blood-born extracellular trypanosomes (Radwanska, et al. 2008). The study demonstrated an early increase in several B cell populations in the spleen associated with the parasitemia peak and followed by a rapid disappearance of B cells from the spleen marginal zone, rendering the immune system unable to mount a long-lasting protective humoral response against re-infections with trypanosomes and to establish immune memory responses against other irrelevant pathogens (Radwanska, et al. 2008). Similarly, *Trypanosoma*-induced B cell depletion from the bone marrow as well as the periphery was also reported after experimental infection of mice with *T. congolense* (Obishakin, et al. 2014). In the present study, looking for an explanation for the reduced B cell count in the blood of diseased camels, one may discuss two possible mechanisms, including infection-induced modulation of B cell production and differentiation in the primary immune organs and a direct or indirect effect of the parasite on B cell viability. To address the first hypothesis, experimental infections of camels are required with subsequent characterization of the whole B cell compartment in the bone marrow, the spleen, and peripheral blood. Although previous studies in mice support a negative effect of *T. brucei* on all B cell developmental stages in the bone marrow (Bockstal, et al. 2011), the investigation of this approach in camel is, however, limited by the

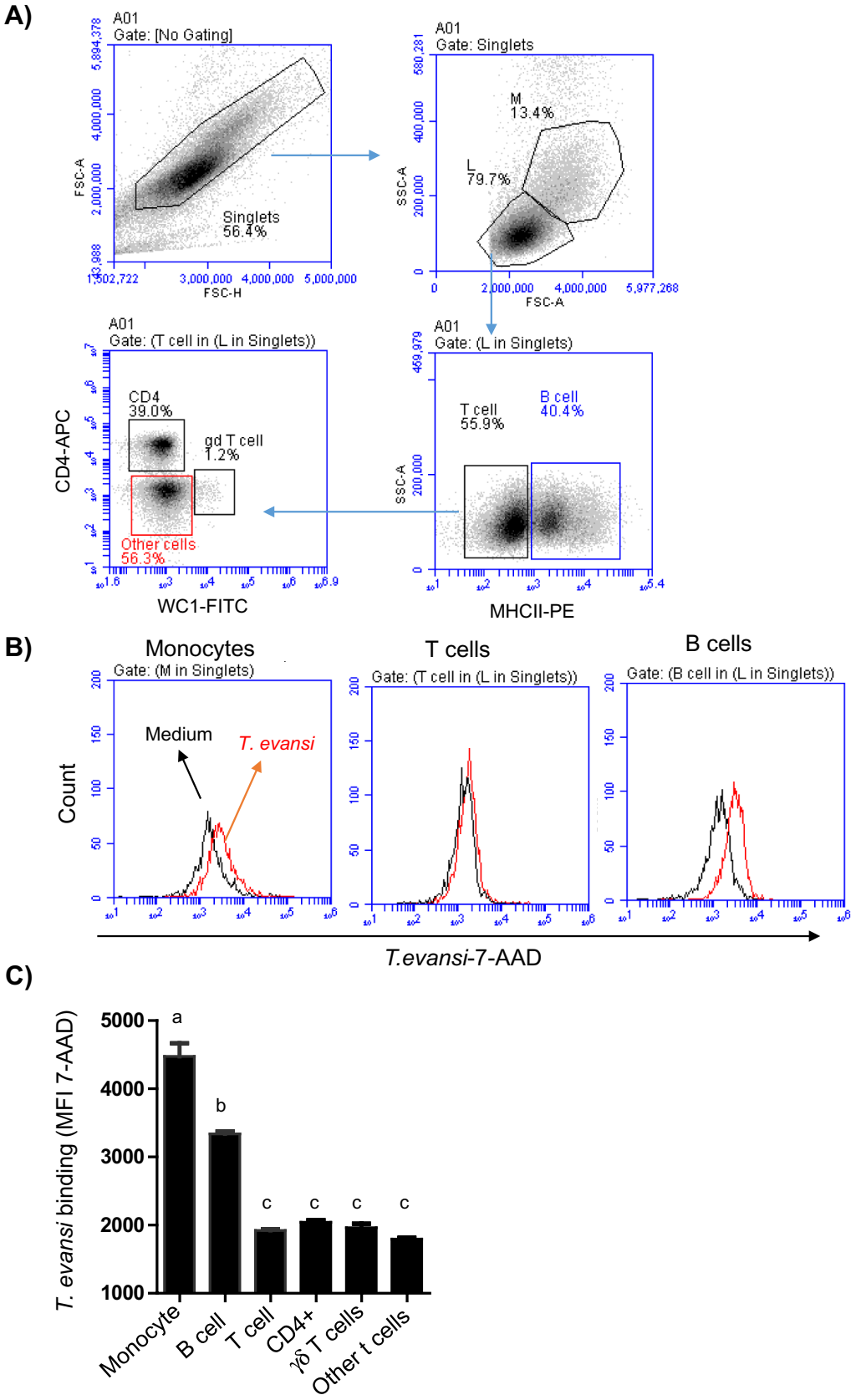
A)
A01
Gate: [No Gating]
FSC-A
FSC-H
Singlets
56.4%
A01
Gate: Singlets
SSC-A
FSC-A
M
13.4%
L
79.7%
A01
Gate: (T cell in (L in Singlets))
CD4-APC
WC1-FITC
CD4
39.0%
gd T cell
1.2%
Other cells
56.3%
A01
Gate: (L in Singlets)
SSC-A
MHCII-PE
T cell
55.9%
B cell
40.4%
B)
Monocytes
Gate: (M in Singlets)
T cells
Gate: (T cell in (L in Singlets))
B cells
Gate: (B cell in (L in Singlets))
Count
Medium
T. evansi
T.evansi-7-AAD
C)
T. evansi binding (MFI 7-AAD)
5000
4000
3000
2000
1000
a
b
c
c
c
c
Monocyte
B cell
T cell
CD4+
γδ T cells
Other t cells

◂**Fig. 5** Differential binding of *T. evansi* to camel lymphocyte subsets. Separated PBMC were labeled with mAbs to CD4, WC1, and MHCII and labeled cells were incubated with whole *T. evansi* parasites stained with 7-AAD. (**A**) Gating strategy of camel PBMC. After the exclusion of cell duplicates in a FSC-A against FSC-H gate, lymphocytes (L) were differentiated from monocytes (M) based on their FSC and SSC properties. Camel T cells and B cells were identified based on the expression of MHCII molecules. T helper cells and γδT cells, and other lymphocytes were identified based on the differential expression of CD4 and WC1. (**B**) Representative histograms of the comparative binding potential of *T. evansi* to camel monocytes, T cells, and B cells determined by the increase in 7-AAD fluorescence intensity of gated cells. (**C**) The binding potential of *T. evansi* to monocytes, T cells, B cells, T helper cells, γδ T cells, and other T cells were calculated as the mean fluorescence intensity (MFI) of 7-AAD and presented graphically. Different small letters indicate significantly different values ($p < 0.05$)

lack of antibodies to cell markers of B cell subsets and their differentiation stages in camels. To prove the second possibility, cell viability analysis of camel PBMC incubated in vitro with *T. evansi* whole parasites revealed a higher fraction of B cells that were positive for Annexin V and Propidium Iodide, indicating *Trypanosoma*-induced apoptosis and necrosis of camel B cells. In an ex vivo setting, Bockstal, et al. (2011) blocked the infection-induced B cell apoptosis by preventing the direct contact between *T. brucei* surface coat and mouse B cells using a VSG-specific nanobody (Bockstal, et al. 2011). In the present study, purified *T. evansi* Ro Tat 1.2 antigen was unable to induce B cell apoptosis, suggesting that trypanosomal antigens other than the VSG Ro Tat 1.2 are responsible for the pro-apoptotic effect on camel B cells or a purification-induced change in the antigenic structure or conformation of the VSG antigen rendering it unable to stimulate B cell apoptosis. *Trypanosoma*-induced B-cell apoptosis has previously also been reported to occur in experimental infections with extracellular and intracellular parasites. The mechanisms reported for *Trypanosoma*-induced B cell apoptosis include Fas/Fas Ligand interactions (Zuniga et al. 2002), caspase-7 activation, and cleavage of phospholipase Cγ1 (Dos Santos, et al. 2020) in the case of *T. cruzi* infections as well as *T. brucei*-induced caspase 3 activation (Radwanska, et al. 2008). Additionally, Frenkel et al. (2016) confirmed the association between African trypanosomiasis and the loss of humoral immune competence due to the depletion of several subtypes of splenic B cells. The study identified an NK cell activating phenotype in mice experimentally infected with *T. brucei* that was responsible for the selective killing of B cells via antibody-independent, perforin-mediated cytotoxicity (Frenkel et al. 2016). In the dromedary camel, the exploration of the role of NK cells in the *T. evansi*-induced depletion of B cells requires further research. For the identification and enumeration of camel NK cells, cross-reactive mAbs with camel NK cell marker antigens such as the NKp46 or CD57 are essential. Furthermore, the characterization of the trypanosomal antigens and the molecular mechanisms that are involved in the observed pro-apoptotic effect of *T. evansi* antigens on camel B cells could be the focus of future research.

Helper T cells are critical players that decide the outcome of infection with trypanosomes by providing help to B cells for antibody production and isotype switching (Shi et al. 2006; Tellier and Nutt 2013). Especially the generation of IFN-gamma-producing T helper 1 cells was associated with IgM to IgG2a class-switching in B cells and protective humoral responses in mice (Tabel et al. 2008). In addition, some studies reported the involvement of T helper cells in disease pathogenesis and death in mice trypanosomal infections (Liu et al. 2015; Shi, et al. 2006). Evasion of cell-mediated immune responses by trypanosomes has also been reported in some studies (Onyilagha et al. 2014). *Trypanosoma congolense*, for example, suppresses CD4 + T cell proliferation and IFN-gamma production, resulting in higher susceptibility of mice to the parasite (Onyilagha et al. 2018). In the present study, although their number did not differ between healthy and diseased animals, T helper cells were significantly reduced in camels with high anti-*Trypanosoma* antibody levels, indicating a role of these cells in protection or pathogenesis. However, the coincidence of low T helper cell numbers and high anti-trypanosoma antibody levels suggests a T-independent B cell activation and argues against a role for T helper cells in B cell activation and class-switching to IgG.

Conclusions

In conclusion, the present study investigated the immunophenotype of blood leukocytes in camels with the clinical surra and serum antibodies against *T. evansi*. The study demonstrates an inflammatory leukogram with slight leukocytosis, neutrophilia, and monocytosis associated with camel trypanosomosis. Ex vivo and in vitro analysis indicate the potential of *T. evansi* to bind to camel B cells and induce their elimination by apoptosis and necrosis. Together, the higher NLR with the reduced numbers of B cells in the diseased group with reduced numbers of T helper cells in the high antibody level group indicate a suppressive effect of *T. evansi* on both humoral and cellular immunity in camels. In addition, the present study indicates that camel trypanosomosis is still present in the Eastern Province of Saudi Arabia and strengthens the need for detailed epidemiological studies to identify the risk-associated predisposing factors including age, vectors, gender, season, breed, and other diseases.

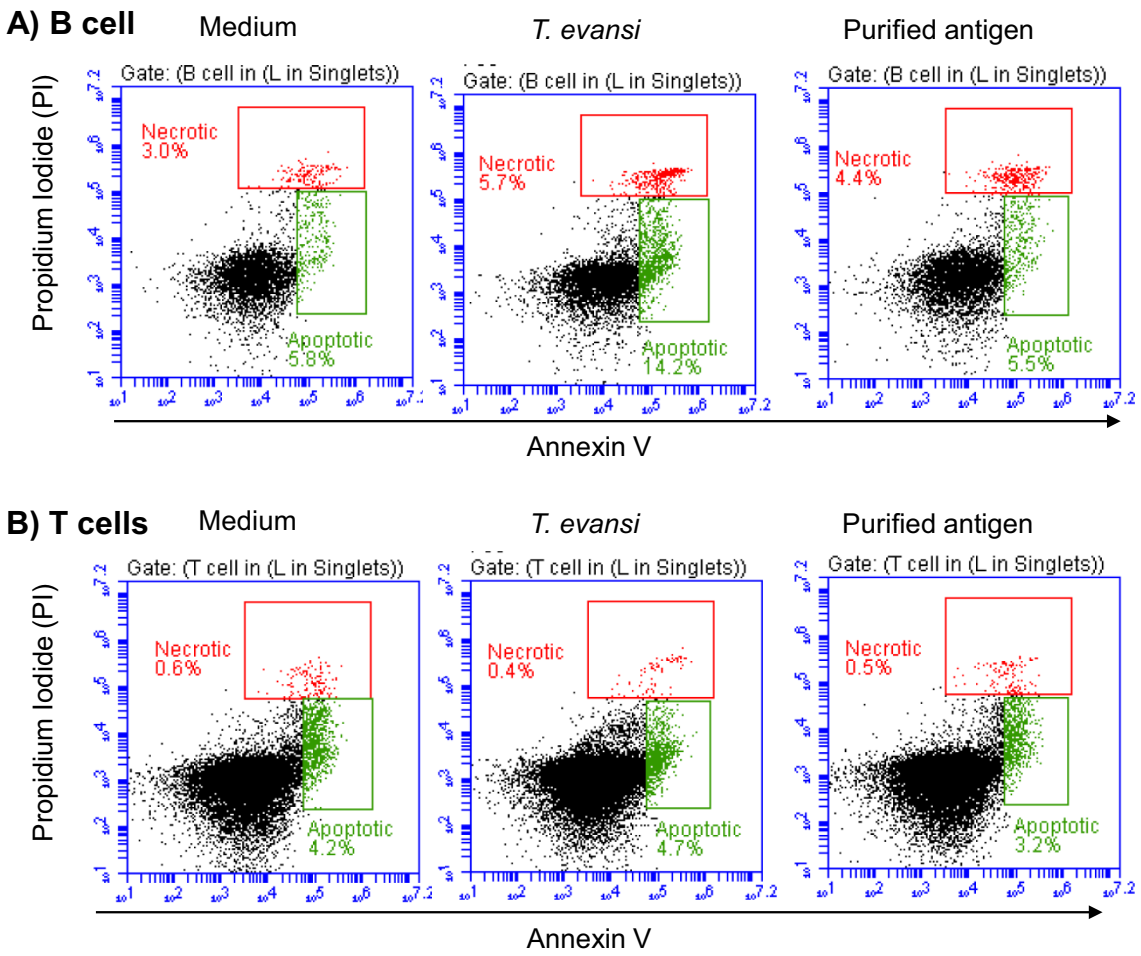
A) B cell
Medium
T. evansi
Purified antigen
Gate: (B cell in (L in Singlets))
Necrotic 3.0%
Apoptotic 5.8%
Necrotic 5.7%
Apoptotic 14.2%
Necrotic 4.4%
Apoptotic 5.5%
Propidium Iodide (PI)
Annexin V
B) T cells
Medium
T. evansi
Purified antigen
Gate: (T cell in (L in Singlets))
Necrotic 0.6%
Apoptotic 4.2%
Necrotic 0.4%
Apoptotic 4.7%
Necrotic 0.5%
Apoptotic 3.2%
Propidium Iodide (PI)
Annexin V

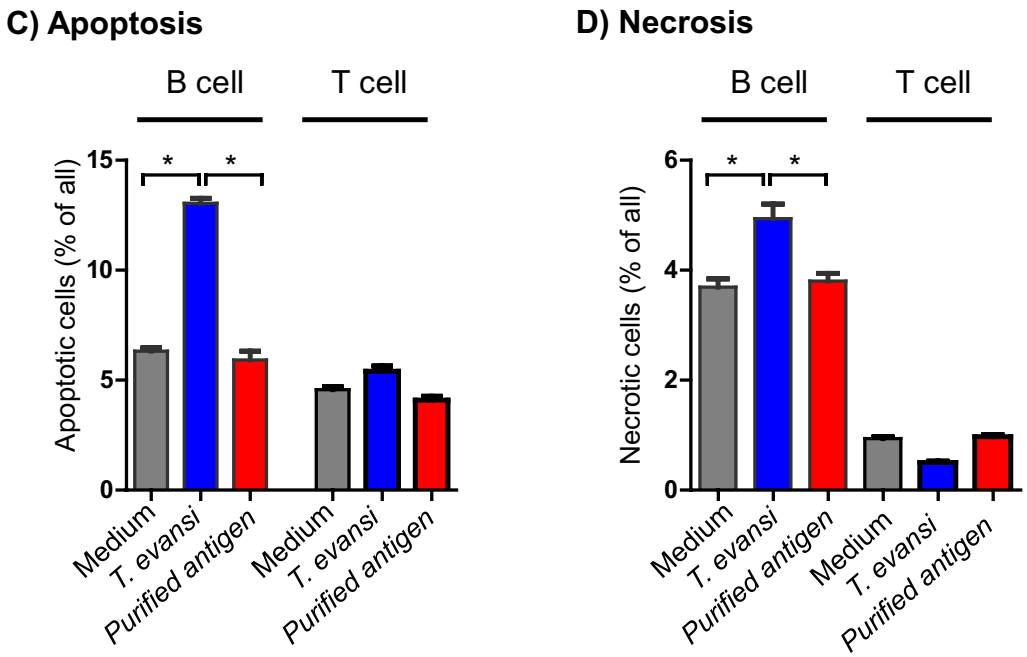
C) Apoptosis
B cell
T cell
Apoptotic cells (% of all)
15
10
5
0
*
*
Medium
T. evansi
Purified antigen
Medium
T. evansi
Purified antigen
D) Necrosis
B cell
T cell
Necrotic cells (% of all)
6
4
2
0
*
*
Medium
T. evansi
Purified antigen
Medium
T. evansi
Purified antigen

◂**Fig. 6** Analysis of cell apoptosis and necrosis. Camel PBMC were incubated in vitro with whole inactivated *T. evansi* parasites or with purified Ro Tat 1.2 antigen for 72h and were labeled with MHCII-APC antibodies for the identification of B cells and T cells. The percentages of apoptotic and necrotic cells were determined after staining with Annexin V and propidium iodide (PI). Annexin V against PI dot plots were used for the identification of apoptotic (Annexin + / PI-) and necrotic (Annexin + / PI +) cells within camel B cells (**A**) and T cells (**B**). The percentage of apoptotic (**C**) and necrotic (**D**) cells within camel B cells and T cells were presented for stimulated and unstimulated cells (n = 4 animals). * indicates significant differences with p value less than 0.5

Such studies would support future control strategies, given the significant impact of the disease on camel health and production.

Supplementary Information The online version contains supplementary material available at https://doi.org/10.1007/s11250-024-04078-9.

Author Contributions Jamal Hussen, Hind Althaqafi, Marc Desquenses, Laurent Hébert, Noof Abdulrahman Alrabiah, Najla K Al Abdulsalam, Abdulaziz Alouffi, and Waleed S. Al-Salem designed the study. Jamal Hussen, Hind Althaqafi, Mohammed Ameer Alalai, and Baraa Falemban collected and analyzed the samples. All authors wrote the first draft of the manuscript. All authors read and approved the final manuscript.

Funding This work was supported through Princess Nourah bint Abdulrahman University Researchers Supporting Project number (PNURSP2024R460), Princess Nourah bint Abdulrahman University, Riyadh, Saudi Arabia.

Data Availability The datasets generated during the current study are available from the corresponding author onon reasonable request.

Declarations

Competing Interests The authors have no relevant financial or non-financial interests to disclose.

Ethics approval This study was performed in line with the principles of the Declaration of Helsinki. Approval was granted by the Ethics Committee of King Faisal University, Saudi Arabia (KFU-REC-2021-DEC -EA000326).

References

Al-Harrasi M et al (2023) Circulation of *Trypanosoma evansi* antibodies and risk variables among dromedary camels in Al Batinah governorates, Sultanate of Oman. Vet Parasitol Reg Stud Reports 40:100863

ALHilal E et al (2023) The Modulation of In Vitro Differentiation of Monocyte-derived Macrophage by *Trypanosoma evansi* Antigens in the Dromedary Camel. World's Vet J 13:587–594

Baral TN et al (2007) Control of *Trypanosoma evansi* infection is IgM mediated and does not require a type I inflammatory response. J Infect Dis 195:1513–1520

Barr DA et al (2021) Flow cytometry method for absolute counting and single-cell phenotyping of mycobacteria. Sci Rep 11:18661

Birhanu H et al (2016) New *Trypanosoma evansi* Type B Isolates from Ethiopian Dromedary Camels. PLoS Negl Trop Dis 10:e0004556

Bockstal V et al (2011) T. brucei infection reduces B lymphopoiesis in bone marrow and truncates compensatory splenic lymphopoiesis through transitional B-cell apoptosis. PLoS Pathog 7:e1002089

Bossard G, Desquesnes M (2023) Validation of in vitro-produced and freeze-dried whole cell lysate antigens for ELISA *Trypanosoma evansi* antibody detection in camels. Vet Parasitol 320:109980

Desquesnes M et al (2013) *Trypanosoma evansi* and surra: a review and perspectives on origin, history, distribution, taxonomy, morphology, hosts, and pathogenic effects. Biomed Res Int 2013:194176

Dos Santos MA et al (2020) Human B cells infected by *Trypanosoma cruzi* undergo F-actin disruption and cell death via caspase-7 activation and cleavage of phospholipase Cgamma 1. Immunobiology 225:151904

Engstler M et al (2007) Hydrodynamic flow-mediated protein sorting on the cell surface of trypanosomes. Cell 131:505–515

Faye B (2020) How many large camelids in the world? A synthetic analysis of the world camel demographic changes. Pastoralism 10:25. https://doi.org/10.1186/s13570-020-00176-z

Frenkel D et al (2016) *Trypanosoma brucei* Co-opts NK Cells to Kill Splenic B2 B Cells. PLoS Pathog 12:e1005733

Gerem B, Hamid M, Assefa A (2020) Prevalence and Associated Risk Factors of *Trypanosoma evansi* in Camels in Ethiopia Based on Parasitological Examinations. Vet Med Int 2020:6172560

Golombieski L et al (2023) Prevalence and Risk Factors Associated With Natural Infection by *Trypanosoma evansi* in Campeiro Horses. J Equine Vet Sci 126:104300

Habeeba S et al (2022) Comparison of Microscopy, Card Agglutination Test for *Trypanosoma Evansi*, and Real-time PCR in The Diagnosis of Trypanosomosis in Dromedary Camels of The Abu Dhabi Emirate, UAE, J. Vet Res 66:125–129

Harris TH, Mansfield JM, Paulnock DM (2007) CpG oligodeoxynucleotide treatment enhances innate resistance and acquired immunity to African trypanosomes. Infect Immun 75:2366–2373

Holland WG et al (2003) The effect of *Trypanosoma evansi* infection on pig performance and vaccination against classical swine fever. Vet Parasitol 111:115–123

Hussen J, Schuberth HJ (2020) Recent Advances in Camel Immunology. Front Immunol 11:614150

Hussen J et al (2023a) Impact of selected bacterial and viral toll-like receptor agonists on the phenotype and function of camel blood neutrophils. Vet Sci 10:154

Hussen J et al (2023b) A flow cytometry study of the binding and stimulation potential of inactivated *Trypanosoma evansi* toward Dromedary camel leukocytes. Pathogens 13:21

Jawalagatti V et al (2023) Expression kinetics of cytokines and the humoral antibody response concerning short-term protection induced by radiation-attenuated *Trypanosoma evansi* in bovine calves. Vaccine 41:1668–1678

Joshi PP et al (2005) Human trypanosomiasis caused by *Trypanosoma evansi* in India: the first case report. Am J Trop Med Hyg 73:491–495

Kim J et al (2023) Recent Progress in the Detection of Surra, a Neglected Disease Caused by *Trypanosoma evansi* with a One Health Impact in Large Parts of the Tropic and Sub-Tropic World. Microorganisms 12:1. https://doi.org/10.3390/microorganisms12010044

Liu G et al (2015) Distinct Contributions of CD4+ and CD8+ T Cells to Pathogenesis of *Trypanosoma brucei* Infection in the

Context of Gamma Interferon and Interleukin-10. Infect Immun 83:2785–2795
Magez S et al (2021) Salivarian Trypanosomes Have Adopted Intricate Host-Pathogen Interaction Mechanisms That Ensure Survival in Plain Sight of the Adaptive Immune System. Pathogens 10:679. https://doi.org/10.3390/pathogens10060679
McGrath JS et al (2017) Analysis of Parasitic Protozoa at the Single-cell Level using Microfluidic Impedance Cytometry. Sci Rep 7:2601
Nguyen HTT et al (2021) Single-cell transcriptome profiling and the use of AID deficient mice reveal that B cell activation combined with antibody class switch recombination and somatic hypermutation do not benefit the control of experimental trypanosomosis. PLoS Pathog 17:e1010026
Obishakin E, de Trez C, Magez S (2014) Chronic *Trypanosoma congolense* infections in mice cause a sustained disruption of the B-cell homeostasis in the bone marrow and spleen. Parasite Immunol 36:187–198
Ogolla KO et al (2023) Spatial-Temporal Variations in Parasitological Prevalence and Host-Related Risk Factors of Camel Trypanosomiasis and Its Vectors in North Eastern Kenya: A Repeated Cross-Sectional Study. J Parasitol Res 2023:7218073
Oldrieve G et al (2021) Monomorphic Trypanozoon: towards reconciling phylogeny and pathologies. Microb Genom 7:000632. https://doi.org/10.1099/mgen.0.000632
Onyilagha C, Uzonna JE (2019) Host Immune Responses and Immune Evasion Strategies in African Trypanosomiasis. Front Immunol 10:2738
Onyilagha C et al (2014) Low-dose intradermal infection with *trypanosoma congolense* leads to expansion of regulatory T cells and enhanced susceptibility to reinfection. Infect Immun 82:1074–1083
Onyilagha C et al (2018) Myeloid-Derived Suppressor Cells Contribute to Susceptibility to *Trypanosoma congolense* Infection by Suppressing CD4(+) T Cell Proliferation and IFN-gamma Production. J Immunol 201:507–515
Otesile EB, Tabel H (1987) Enhanced resistance of highly susceptible Balb/c mice to infection with *Trypanosoma congolense* after infection and cure. J Parasitol 73:947–953
Pays E, Radwanska M, Magez S (2023) The Pathogenesis of African Trypanosomiasis. Annu Rev Pathol 18:19–45
Powar RM et al (2006) A rare case of human trypanosomiasis caused by *Trypanosoma evansi*. Indian J Med Microbiol 24:72–74
Radwanska M et al (2008) Trypanosomiasis-induced B cell apoptosis results in loss of protective anti-parasite antibody responses and abolishment of vaccine-induced memory responses. PLoS Pathog 4:e1000078
Rottcher D, Schillinger D, Zweigarth E (1987) Trypanosomiasis in the camel (Camelus Dromedarius). Rev Sci Tech 6:463–470
Salim B et al (2011) Molecular epidemiology of camel trypanosomiasis based on ITS1 rDNA and RoTat 1.2 VSG gene in the Sudan. Parasit Vectors 4:31
Shegokar VR et al (2006) Short report: Human trypanosomiasis caused by *Trypanosoma evansi* in a village in India: preliminary serologic survey of the local population. Am J Trop Med Hyg 75:869–870
Shi M et al (2006) Experimental African trypanosomiasis: a subset of pathogenic, IFN-gamma-producing, MHC class II-restricted CD4+ T cells mediates early mortality in highly susceptible mice. J Immunol 176:1724–1732
Soehnlein O, Lindbom L (2010) Phagocyte partnership during the onset and resolution of inflammation. Nat Rev Immunol 10:427–439
Tabel H, Wei G, Shi M (2008) T cells and immunopathogenesis of experimental African trypanosomiasis. Immunol Rev 225:128–139
Tellier J, Nutt SL (2013) The unique features of follicular T cell subsets. Cell Mol Life Sci 70:4771–4784
Tran T et al (2009) Towards a new reference test for surra in camels. Clin Vaccine Immunol 16:999–1002
Van Vinh Chau N et al (2016) A Clinical and Epidemiological Investigation of the First Reported Human Infection With the Zoonotic Parasite *Trypanosoma evansi* in Southeast Asia. Clin Infect Dis 62:1002–1008
Wilson, R.T., and Dioli, M., 2021. History of Trypanosomosis in the One-Humped Camel and Development of its Treatment and Cure, with Special Reference to Sudan. Med Res Arch , 9 https://doi.org/10.18103/mra.v9i7.2513
World Health Organization (2005) A new form of human trypanosomiasis in India Description of the First Human Case in the World Caused by Trypanosoma Evansi. Wkly Epidemiol Rec 80:62–63
Zuniga E et al (2002) *Trypanosoma cruzi* infection selectively renders parasite-specific IgG+ B lymphocytes susceptible to Fas/Fas ligand-mediated fratricide. J Immunol 168:3965–3973